Correlation of SD-OCT Features and Retinal Sensitivity in Neovascular Age-Related Macular Degeneration

Florian Sulzbacher,[1] *Christopher Kiss,*[1] *Alexandra Kaider,*[2] *Stefan Eisenkoelbl,*[1] *Marion Munk,*[1] *Philipp Roberts,*[1] *Stefan Sacu,*[1] *and Ursula Schmidt-Erfurth*[1]

Purpose. To correlate retinal sensitivity in patients with neovascular age-related macular degeneration (AMD) with specific characteristics of retinal morphology.

Methods. Thirty eyes of 30 patients presenting with active choroidal neovascularization were examined by spectral domain optical coherence tomography (SD-OCT) and microperimetry (MP-1). Image-processing software was used to match a fundus photographic (FP) MP-1 image with an infrared+OCT SD-OCT image. Each MP test point for retinal sensitivity was positioned at the corresponding SD-OCT location, and the microperimetric results were evaluated.

Results. An intact retinal configuration was associated with a median retinal sensitivity of 15.5 dB (quartiles: 12 dB, 18 dB). The median retinal sensitivities were 0 dB (quartiles: 0 dB, 1 dB) for the neovascular complex, 4 dB (0 dB, 9 dB) for the subretinal fluid, 1 dB (0 dB, 6 dB) for the intraretinal fluid, and 0 dB (0 dB, 3 dB) for intraretinal cysts. Pigment epithelium detachment was associated with a median retinal sensitivity of 3 dB (0 dB, 8 dB), and subretinal drusen had a median value of 8 dB (5 dB, 12 dB). Deep retinal layer analyses gave low median retinal sensitivities of 0 dB (0 dB, 3 dB) for an absent retinal pigment epithelium layer and 1 dB (0 dB, 5 dB) for an absent photoreceptor layer.

Conclusions. Superimposition of morphological SD-OCT features and microperimetric retinal sensitivity allowed exact determination of the differential impact of retinal alteration on the corresponding sensitivity. Individual OCT-related indicators of neurosensory integrity were distinctly correlated with visual function. "Morphofunctional" findings could be relevant as prognostic factors and for (re)treatment decisions. (https://www.clinicaltrialsregister.eu/ number, 2006-005684-26.) (*Invest Ophthalmol Vis Sci.* 2012;53:6448–6455) DOI:10.1167/iovs.11-9162

Neovascular age-related macular degeneration (AMD) is characterized by a series of morphological changes in the retina, below the retina, and at the level of the RPE. These changes include choroidal neovascularization (CNV), sub- and intraretinal exudation, and pigment epithelium detachment. Fluorescein angiography (FA) has been used for classification of CNV as classic or occult on the basis of the Macular Photocoagulation Study criteria. However, the ANCHOR and MARINA trials did not show a difference in treatment response between these two lesion compositions.[1,2] A new classification for AMD based on multimodal imaging defines type 1 CNV as neovascularization observed beneath the RPE monolayer and type 2 neovascularization as neovascular tissue that has penetrated the RPE/Bruch membrane complex and proliferated in the subretinal space. This classification is consistent with the Gass classification.[3] Type 3 suggests an intraretinal origin of neovascularization.[4]

State-of-the-art spectral domain optical coherence tomography (SD-OCT) enables histological-like visualization of retinal morphology and detailed imaging of the pigment epithelium and photoreceptor layer.[5] To improve our understanding of the pathophysiology of AMD, it is desirable to assess morphological alterations and their corresponding retinal function. It is all the more important because effective therapies have led to stabilization and improvement of vision.

Present therapies include thermal photocoagulation, photodynamic therapy using verteporfin, and retinal pharmacotherapy that inhibits vascular endothelial growth factor.[6] For appropriate evaluation of available therapies, crucial functional parameters must be identified. An accurate, repeatable, and topographically specific evaluation of central retinal function can be obtained using fundus-related microperimetry, which gives a retinal sensitivity map registered with a color fundus image.[7,8] An exact overlay of such functional mapping with high-resolution images of the retina can reveal the functional impact of microstructural alterations in vivo. The present study uses the concept of structure–function correlation by an exact manual superimposition of the retinal sensitivity map to OCT data using a spectral domain imaging device and the Micro Perimeter 1 (MP-1, Nidek, Gamagori, Japan). Previous studies have highlighted the accuracy of coregistration of functional mapping with retinal imaging and identified consistent associations between high-resolution imaging and visual function.[9] Loss of the inner segment–outer segment (IS/OS) layer has shown a significant association with poor retinal sensitivity.[10] Increased total volume of the outer nuclear layer (ONL) has been shown to be associated with decreased visual acuity (VA). However, the total volume of intraretinal cystoid spaces (IRC) has not shown a correlation with visual acuity.[11]

Central retinal thickness (CRT) and visual acuity are poorly correlated because of the diversity of factors associated with CRT.[12] Current retreatment strategies in AMD target specific OCT findings, particularly the elimination of intra- or subretinal fluid. To date, change in best-corrected VA (BCVA) (defined as a loss of 5 letters) has been included as a functional criterion for

From the [1]Department of Ophthalmology, and [2]Center for Medical Statistics, Informatics, and Intelligent Systems, Section for Clinical Biometrics, Medical University of Vienna, Vienna, Austria.

Presented at the Association for Research in Vision and Ophthalmology Annual Meeting, Fort Lauderdale, Florida, May 2010.

Submitted for publication November 25, 2011; revised May 15 and July 12, 2012; accepted August 18, 2012.

Disclosure: **F. Sulzbacher**, None; **C. Kiss**, None; **A. Kaider**, None; **S. Eisenkoelbl**, None; **M. Munk**, None; **P. Roberts**, None; **S. Sacu**, None; **U. Schmidt-Erfurth**, None

Corresponding author: Christopher Kiss, Department of Ophthalmology & Optometry, Medical University of Vienna, Waehringer Guertel 18-20, A-1090 Vienna, Austria; christopher.kiss@meduniwien.ac.at.

Investigative Ophthalmology & Visual Science, September 2012, Vol. 53, No. 10

retreatment.[13] However, the inability to read or recognize details in everyday tasks in AMD has a substantial effect on patients' quality of life. Despite the presence of a central scotoma, some patients can handle their disability fairly well if eccentric fixation is well established.[14]

It can be difficult to determine if improvement of reading is based on treatment success or on learning eccentric fixation because the size of absolute and relative scotomas have a variable correlation with reading speed and print size.[15] Therefore, retinal sensitivity assessed by fundus-related microperimetry may provide more reliable insight into macular function deficiencies than by distance VA or reading performance. Accurate measurement of functional deficiency and determination of the responsible morphological correlate enable a better understanding of AMD by detecting the underlying cause of vision loss, which allows a precise determination of the functional stage and may improve the chance of treatment success.

For the current study, clearly defined OCT features, such as retinal pigment epithelium detachment (PED), sub- and intraretinal fluid (SRF, IRF), neovascular complex (NVC), intraretinal cysts (IRC), hard exudates (HE), and subretinal drusen (SRD) were measured and compared with local retinal function. In addition, the level of photoreceptor alteration and condition of the RPE layer unrelated to exudation were also evaluated.

Patients and Methods

Our study was conducted at the Department of Ophthalmology of the Medical University of Vienna. It was approved by the local ethics committee and adhered to the Declaration of Helsinki. Every patient gave written informed consent before study inclusion. Thirty eyes of 30 patients with active subfoveal choroidal neovascularization (9 classic, 10 minimally classic, 11 occult) secondary to AMD were evaluated. Each patient underwent a complete clinical examination by slit-lamp biomicroscopy, ophthalmoscopy, and fundus photography, as well as by FA and SD-OCT. The Micro Perimeter 1 (MP-1, Nidek) was used to perform fundus-monitored microperimetry. Microperimeter settings were based on a 4-2-1 staircase strategy with Goldmann III-size stimuli (stimulus intensity range, 0–20 dB). A Cartesian grid with 33 stimulus locations covering the central area of $12 \times 12^\circ$ was selected, while a 3° ring was used as the fixation target.

Measurements and Imaging Preparation

OCT images were obtained with a spectral domain imaging device (Spectralis HRA + OCT; Heidelberg Engineering, Heidelberg, Germany). The infrared+OCT tool of the Spectralis OCT was used to assess a horizontal volume scan involving 49 scans with 25 frames. The scan diameter was 6000 μm.

VirtualDub (Ver.1.8.6) software (available at http://www.virtualdub.org) and Paint.NET (Ver. 3.36) software (http://www.getpaint.net) was used to manually superimpose MP-1 color fundus photographic (FP) images, including the sensitivity map of each eye on corresponding infrared images of the SD-OCT. To ensure correct measurement, retinal vessel landmarks were matched manually; subsequently, raster scans were superimposed over the fundus photographs to create FP and OCT composites. For point-to-point superimposition, Image J software (available at http://rsbweb.nih.gov/ij/, National Institute of Health, Bathesda, MD) was used to transfer each stimulus location in the sensitivity map to the corresponding location of the SD-OCT B-scan true to scale. The scale for the superimposed FP sensitivity map was 11 pixels per 200 μm and 34 pixels per 200 μm for the OCT scale, which was based on the assumption that the scale as shown in the bottom right corner of each Heidelberg image was accurate (Fig. 1).

Image Analyses

After transferring each stimulus location of the FP to the SD-OCT B-scan for each test point location, the status of the SD-OCT morphology was categorized according to the following pathological findings: NVC, fibrovascular pigment epithelium detachment (FPED), serous pigment epithelium detachment (SPED), SRF, IRF, IRC, HE, and SRD. Simultaneously, the integrity of IS/OS of the photoreceptors, the RPE, and the external limiting membrane (ELM) were evaluated by the following strategy. The IS/OS was graded as complete if the hyperreflective line (interface) between the IS/OS was present, as discontinuous if the hyperreflective line (interface) between the IS/OS was interrupted and the segments were only partly visible, or as completely absent. The RPE layer was graded as complete if the hyperreflective band was continuous, as discontinuous if the RPE was disrupted and only partly visible, or as absent if no hyperreflectivity was visible. The ELM was graded as present or absent. The retina was graded as intact if the RPE layer showed a homogeneous hyperreflective band, the IS/OS was divided by a hyperreflective line, and the ELM was clearly discernible. Furthermore, none of the mentioned pathological findings must be present.

The manual superimposition procedure and the OCT reading were reviewed by two experienced readers (P.R. and S.E.). Smaller regions of pathological features (i.e., cysts, exudates, drusen, or IS/OS boundary loss) were considered to be present if they appeared exactly above a test point. To avoid misleading results, light stimulus locations at the margins of that region were not considered. Most cases showed very good agreement in correct alignment of image superimposition and light stimulus transfer. Some remaining concerns were possible inaccuracies of the devices themselves; the Spectralis was observed to sometimes miss the targeted scan line. The manual superimposition procedure also may have induced inaccuracies. For that reason, the appearance of the retinal vessels in both modalities before and after superimposition was used for ensuring correct alignment and measurement. Considering these points, we estimate a high degree of accuracy in our investigation.

For each morphological alteration, retinal sensitivity results were identified and statistically evaluated. Retinal sensitivity values were described by median and quartile values. To identify the diagnostic relevance of the specific SD-OCT morphology, positive predictive values (PPV) with respect to every observed retinal sensitivity cutoff value (0–20) were evaluated. For this purpose, we calculated for each OCT finding the proportion of test points with retinal sensitivity values less than or equal to the respective cutoff values. For each OCT finding, ANOVA models were created to compare the respective retinal sensitivity values with those of intact retina. Multiple measurements within the same patient were considered appropriately by including the patient factor in the ANOVA models. Within-patient variances were compared across patient variances for each OCT finding. Furthermore, for each case, Spearman's r coefficient was used to correlate the central retinal thickness value as assessed by SD-OCT with the corresponding central retinal sensitivity value. SAS software (version 9.2, SAS Institute Inc., Cary, NC) was used to perform statistical analysis.

Results

Quantitative Correlation of OCT Features and Retinal Sensitivity

The correlation of the central retinal thickness values with the central retinal sensitivity values gave a Spearman r value of -0.509 ($P = 0.004$), indicating a rather strong negative correlation (Fig. 2). The negative value of the correlation coefficient indicates a tendency of increasing central retinal sensitivity levels in eyes with lower central retinal thickness.

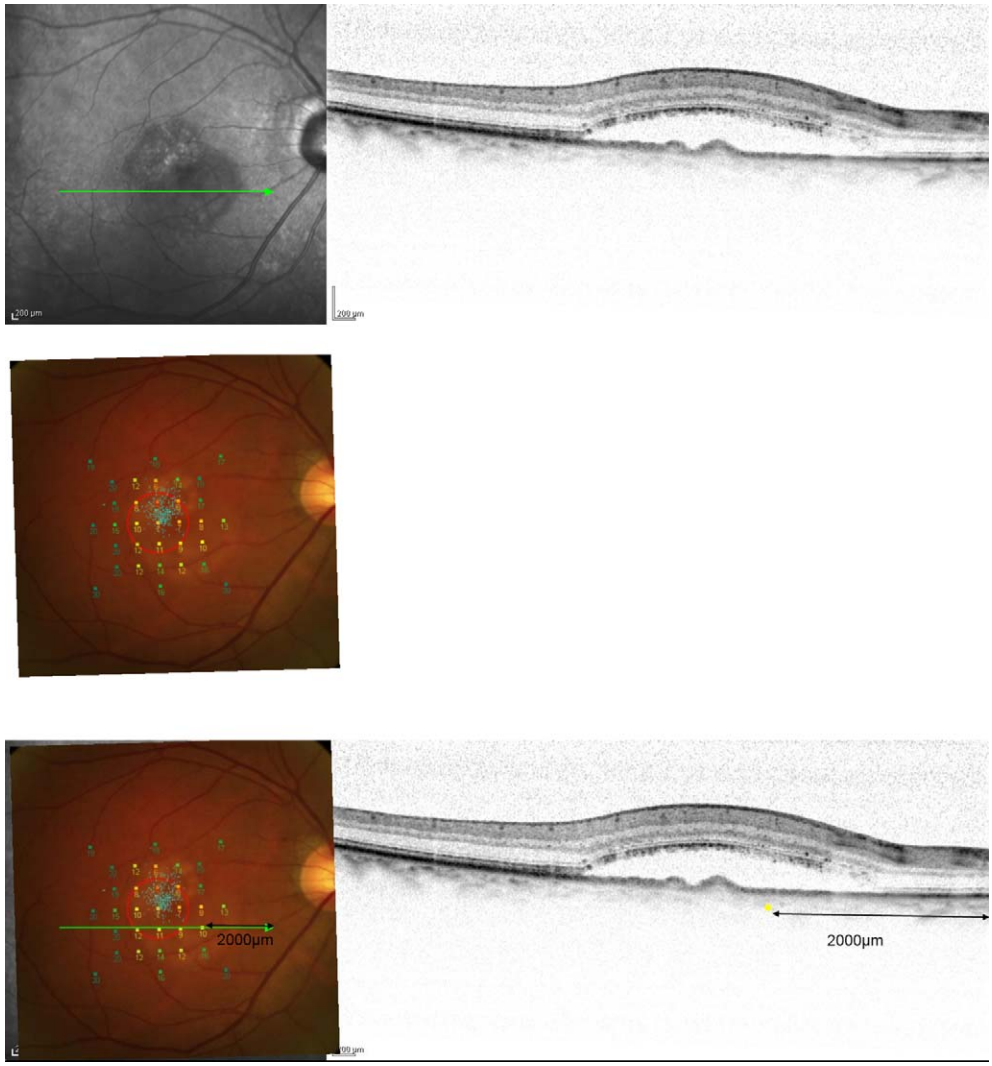

Figure 1. Processing of SD-OCT and fundus sensitivity map images (*top*). The corresponding infrared+OCT image of SD-OCT was generated by VirtualDub software and imported to Paint.NET software (*middle*). Subsequently, the fundus photograph with the sensitivity map was cut and matched to the infrared picture according to retinal landmarks (*bottom*). Finally, the OCT scan shown by the green arrow at locations of the light presentation was selected and matched with the adapted fundus sensitivity map. Subsequently, Image J software was used to transfer each stimulus location in the sensitivity map to the corresponding location of the B-scan in SD-OCT true to scale. For further explanation, see Patients and Methods.

Qualitative Correlation of OCT Features and Retinal Sensitivity

A total of 978 focal retinal sensitivity locations in 30 eyes with neovascular AMD were evaluated according to their morphological correlates in the B-scan of the SD-OCT. The morphological entities and the corresponding sensitivity values are presented in Figures 3A to E. For comparison, the functional deficiencies of the OCT features are shown in Figure 4. An intact retinal configuration was associated with a median retinal sensitivity of 15.5 dB (quartiles: 12 dB, 18 dB). The within-eyes variance was 1.8 times higher than the across eyes variance.

Macular Sensitivity Associated with NVC

NVCs were present at 98 locations in 18 eyes, and had a median value of 0 dB (quartiles: 0 dB, 1 dB) and a PPV of 81% for a retinal sensitivity cutoff value of 2 dB, which meant that 81% of the NVC findings had a retinal sensitivity of less than or equal to 2 dB. ANOVA showed a statistically significant difference between NVC and intact retina ($P \leq 0.0001$), with a mean difference of 12.4 dB (95% confidence interval [CI] = 11.5–13.3).

Macular Sensitivity Associated with Retinal Fluid

SRF was detected at 166 locations of 21 eyes, and the median retinal sensitivity was 4 dB (0 dB, 9 dB), with a PPV of 83% for a cutoff value of 11 dB. ANOVA showed a statistically significant difference between SRF and intact retina ($P \leq 0.0001$), with a mean difference of 8.2 dB (95% CI = 7.1–9.3).

IRF was detected at 176 locations of 23 eyes, and the median retinal sensitivity was 1 dB (0 dB, 6 dB), with a PPV of 83% for a cutoff value of 7 dB. ANOVA showed a statistically significant difference between IRF and intact retina ($P \leq 0.0001$), with a mean difference of 10.4 dB (95% CI = 9.3–11.5). IRC were detected at 114 locations in 19 eyes, and the median retinal sensitivity was 0 dB (0 dB, 3 dB). ANOVA showed a statistically significant difference between IRC and

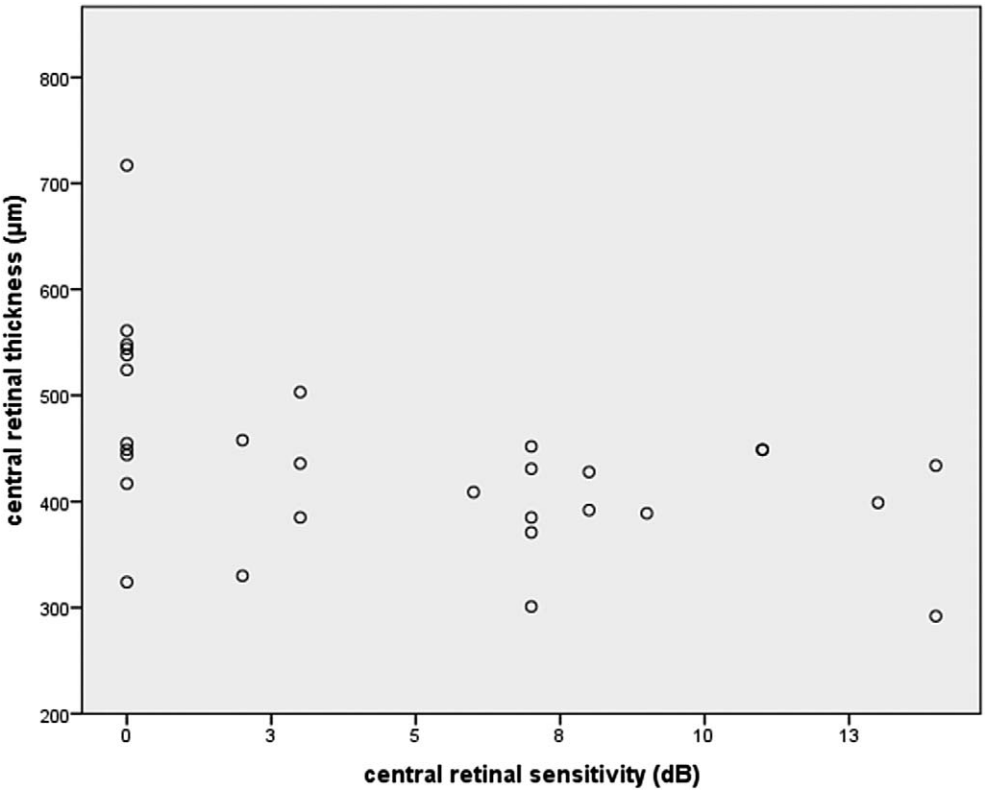

Figure 2. Correlation of central retinal sensitivity in decibels (x-axis) with central retinal thickness in microns (y-axis) gave a Spearman *r* value of –0.509 ($P = 0.004$), indicating a rather strong negative association.

intact retina ($P \leq 0.0001$), with a mean difference of 9.3 dB (95% CI = 8.2–10.5).

Macular Sensitivity Associated with a PED and SRD

A SPED was detected at 81 locations of 15 eyes and had a median retinal sensitivity of 2 dB (0 dB, 6.5 dB). ANOVA showed a statistically significant difference between SPED and intact retina ($P \leq 0.0001$), with a mean difference of 9.3 dB (95% CI = 8.0–10.5). A FPED was detected at 161 locations of 18 eyes and had a median retinal sensitivity of 5 dB (0.5 dB, 10 dB). ANOVA showed a statistically significant difference between SPED and intact retina ($P \leq 0.0001$), with a mean difference of 7.8 dB (95% CI = 6.5–9.0).

The presence of SRD resulted in a median perception value of 8 dB (5 dB, 12 dB) assessed at 160 locations in 17 eyes. ANOVA showed a statistically significant difference between SRD and intact retina ($P \leq 0.0001$), with a mean difference of 4.0 dB (95% CI = 11.5–13.3). The individual results are shown in Table 1, and the combined results are shown in Table 2.

Deep Retinal Layers and Sensitivity

Retinal sensitivity results of deep retinal layer analyses, which indicated the conditions of the RPE layer, the IS/OS layer, and the ELM layer, are shown in Figure 5.

Qualitative Correlation of OCT Features and Retinal Sensitivity According to Deep Retinal Layers Status

At 58 locations associated with NVC (59%), the RPE layer was graded as absent, and the median retinal sensitivity was 0 dB (0 dB, 0 dB), whereas, in 41%, the RPE layer was graded as discontinuous, and the median retinal sensitivity was 0 dB (0 dB, 5 dB). At 86 locations associated with NVC (88%), the IS/OS was graded as absent, and the median retinal sensitivity was 0 dB (0 dB, 1 dB), whereas in 12%, the IS/OS was graded as discontinuous, and the median retinal sensitivity was 0 dB (0 dB, 4 dB). At 93 locations associated with NVC (95%), the ELM was graded as absent, and the median retinal sensitivity was 0 dB (0 dB, 1 dB), whereas in 5%, the ELM layer was graded as complete, and the median retinal sensitivity was 0 dB (0 dB, 4.5 dB).

At 47 locations associated with SRF (28%), the RPE layer was graded as absent, and the median retinal sensitivity was 0 dB (0 dB, 8 dB), whereas in 66%, the RPE layer was graded as discontinuous, and the median retinal sensitivity was 5 dB (0 dB, 10 dB). The RPE layer was graded as complete in 6% and the median retinal sensitivity was 6.5 dB (4 dB, 13.5 dB). At 61 locations associated with SRF (37%), the IS/OS was graded as absent, and the median retinal sensitivity was 0 dB (0 dB, 3.5 dB), whereas in 60%, the IS/OS was graded as discontinuous, and the median retinal sensitivity was 7 dB (0.5 dB, 12 dB). In 3%, the IS/OS was graded as complete, and the median retinal sensitivity was 12 dB (10 dB, 16.5 dB).

At 70 locations associated with SRF (42%), the ELM was graded as absent, and the median retinal sensitivity was 0.5 dB (0 dB, 7 dB), whereas in 58%, the ELM was graded as present, and the median retinal sensitivity was 7 dB (0 dB, 11 dB).

At 41 locations associated with PED (17%), the RPE layer was graded as absent, and the median retinal sensitivity was 1 dB (0 dB, 4.5 dB), whereas in 77%, the RPE layer was graded as discontinuous, and the median retinal sensitivity was 4 dB (0 dB, 9 dB). In 6%, the RPE layer was graded as complete, and the median retinal sensitivity was 7 dB (4.5 dB, 11 dB). At 148 locations associated with PED (62%), the IS/OS was graded as absent, and the median retinal sensitivity was 2 dB (0 dB, 5 dB),

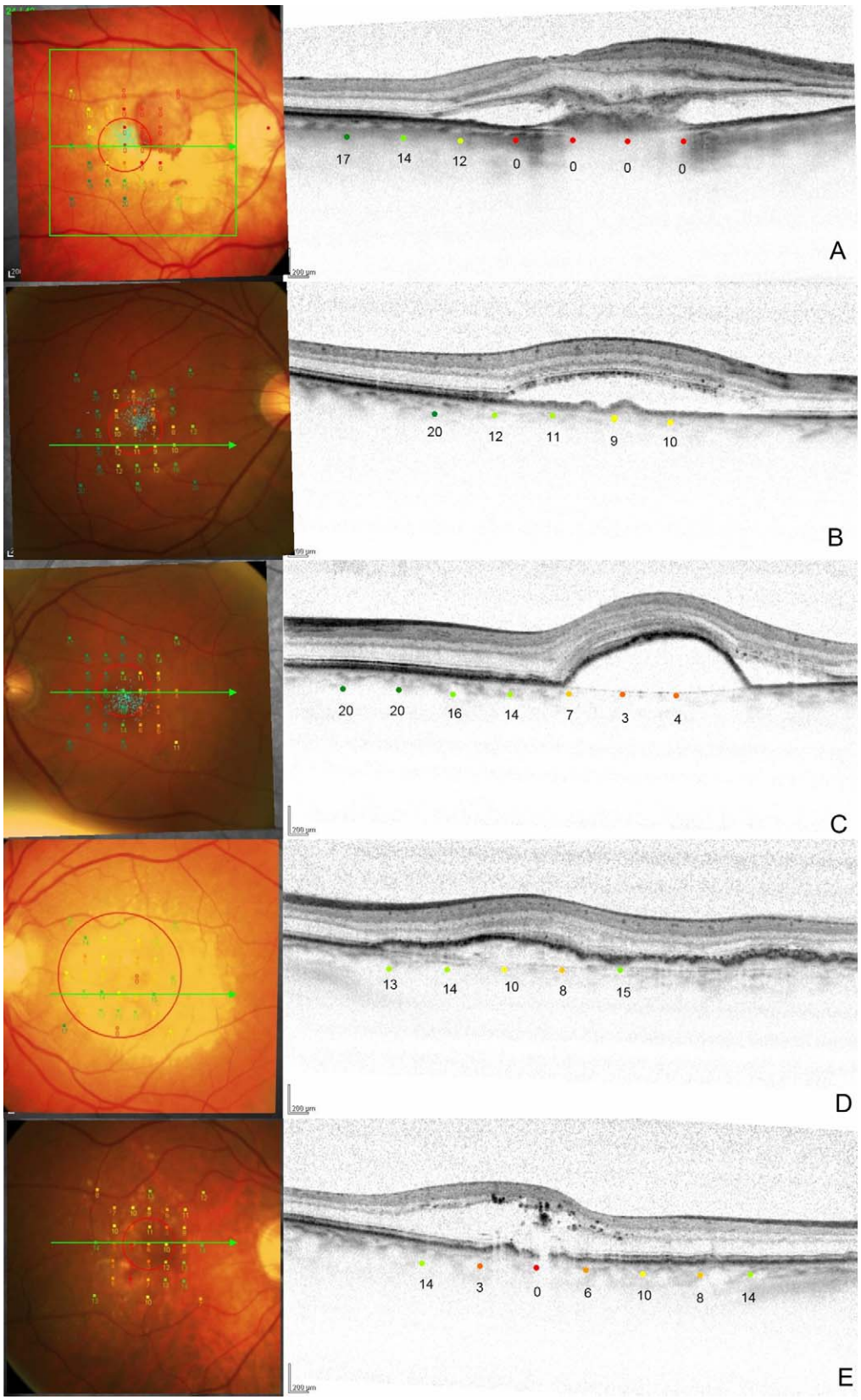

Figure 3. SD-OCT B scans with corresponding retinal sensitivity values according to the superimposed fundus image of the MP-1 microperimeter showing a neovascular complex and subretinal fluid (*panel A*), subretinal fluid and subretinal drusen (*panel B*), a serous pigment epithelium detachment (*panel C*), a fibrovascular pigment epithelium detachment (*panel D*), and intraretinal fluid with hard exudates (*panel E*). Zero decibel marked with a red spot implicates no threshold perception; 20 decibel marked with a green spot implicates the best possible function.

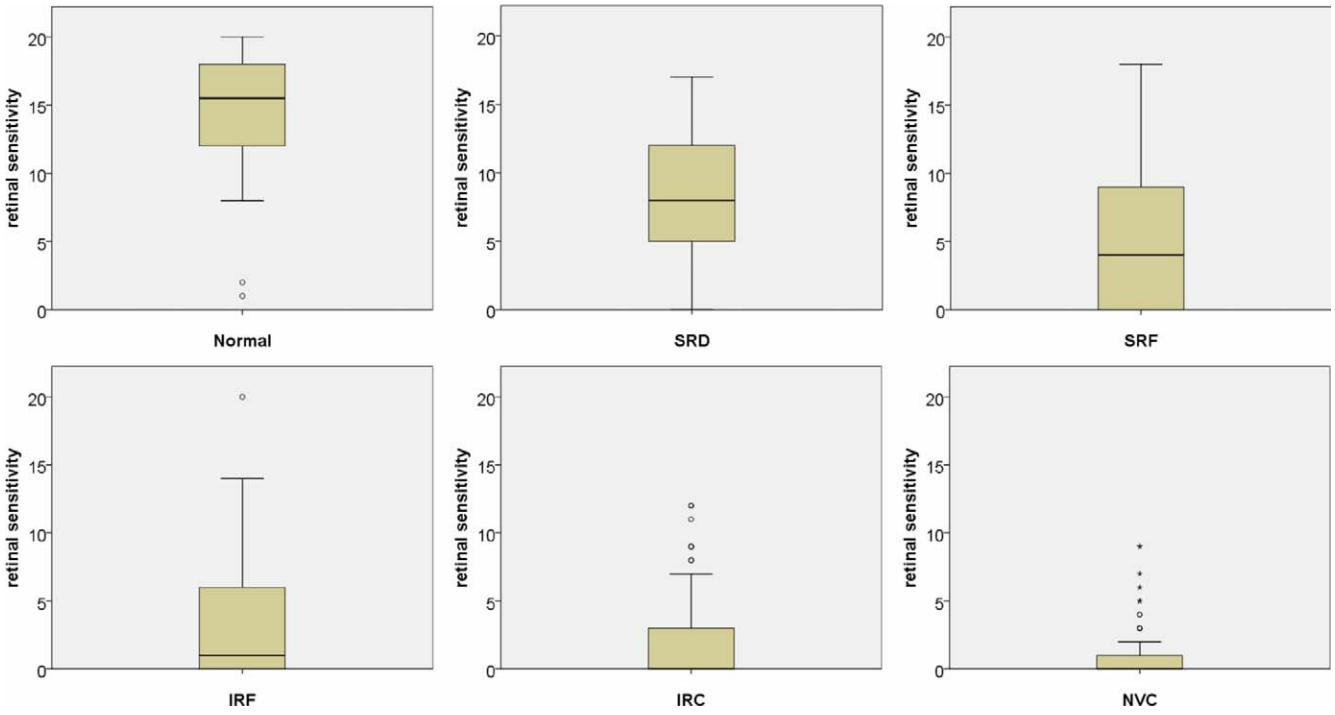

Figure 4. Box plots representing the focal retinal sensitivity in decibels from 0 to 20 (y-axis) associated with each morphological entity. Normal indicates normal retinal configuration.

whereas in 36%, the IS/OS was graded as discontinuous, and the median retinal sensitivity was 8 dB (3 dB, 12 dB). In 2%, the IS/OS was graded as complete, and the median retinal sensitivity was 13.5 dB (9.5 dB, 17 dB). At 150 locations associated with PED (63%), the ELM was graded as absent, and the median retinal sensitivity was 2 dB (0 dB, 7 dB), whereas in 37%, the RPE layer was graded as present, and the median retinal sensitivity was 7 dB (3 dB, 12 dB).

Discussion

The purpose of our study was to quantify the loss in retinal sensitivity typically associated with distinct morphological changes in patients with neovascular AMD. Two state-of-the-art modalities were used to assess the structure–function relationship on the basis of topographic correlation using image-processing software. This procedure allowed a point-to-point analysis of the morphological data and corresponding functional impact of microstructural alterations. Our investigation focused on characteristic OCT findings that were well defined and analyzed by OCT reading centers. The degree of severity of outer retinal damage and characteristic OCT findings were assigned to a distinct degree of functional damage. The response to treatment and retreatment could be evaluated more accurately with the integration of functional data because there are doubts that OCT measurements alone are robust surrogate markers for visual function and because VA testing exclusively reveals foveal function but does not provide a functional map of the retina.[16]

In our evaluation of treatment-naive CNV lesions due to AMD, we were able to show that NVC sites demonstrated complete macular functional loss independently if cysts or IRF were also present. Detailed analyses at those sites showed disrupted RPE and absent photoreceptor integrity (Fig. 3A). Sites of macular edema presenting as SRF, IRF, or IRC alone were characterized by a moderate loss of retinal function (Fig. 3), with no marked differences in the degree of severity between the compartment locations (Table 1), whereas the combined manifestation of SRF and IRF was associated with severe macular functional loss (Table 2). At sites of macular edema, RPE, IS/OS and ELM showed varying conditions; functionally, there was a trend toward higher retinal sensitivity in lesions with discernible and continuous layers. In diabetic macular edema,[17] significant differences in macular function dependent on morphological manifestations were found, with

Table 1. Median Retinal Sensitivity and Quartiles in dB of the Individual OCT Alteration

Finding	Median Sensitivity (Quartiles)	Test Points	Eyes
NVC	1 (0, 5)	25	8
SRF	5.5 (0, 11)	90	18
IRF	7 (0, 9)	34	14
PED	7 (2, 10)	102	18
SPED	3 (0, 7)	28	9
FPED	7 (2, 11)	71	13
IRC	8 (3, 9)	12	5
SRD	9 (5, 13)	94	15
Normal	15.5 (12, 18)	114	22

normal, normal retinal configuration.

Table 2. Median Retinal Sensitivity and Quartiles in dB of the Corresponding Finding with Combined Morphological Alterations

Findings	Median Sensitivity (Quartiles)	Test Points	Eyes
NVC + IRC	0 (0, 0)	13	6
SRF + SRD	7 (0, 10.5)	9	5
IRF + SRF	1.5 (0, 6)	11	6
PED + IRC	0 (0, 2)	31	8
PED + IRF	1.5 (0, 6)	10	5
IRF + HE	3 (0, 5)	15	5
PED + SRF	7 (2, 13)	27	9

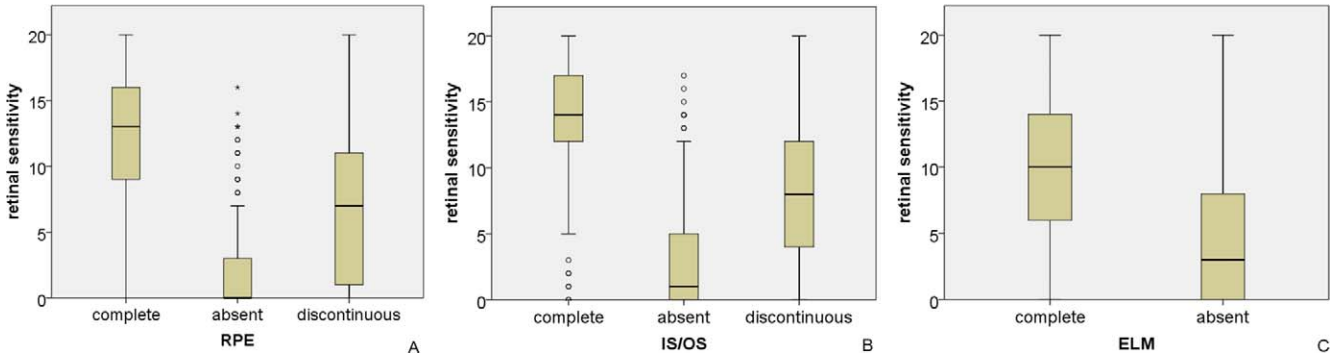

Figure 5. Box plots representing the focal retinal sensitivity in decibels from 0 to 20 (y-axis) associated with the condition of deep layers. *Panel A:* the RPE; *panel B:* the IS/OS of the photoreceptors; and *panel C:* the ELM based on the whole collective.

serous retinal detachment and giant outer nuclear layer (ONL) cysts having a greater negative impact on macular function and small ONL cysts and diffuse swelling affecting macular function to a lesser degree.

Furthermore, we found that isolated PED was associated with variable macular sensitivity; that is, serous PED presented with greater deficiency of macular function than did fibrovascular PED (Fig. 3). The combination of PED with IRF and/or cysts was associated with marked functional loss, whereas the combination of PED and SRF had a lower negative impact on macular function (Table 2). However, in combined findings, the number of test points and examined eyes was low, which might have had an impact on the results as well. Keane et al.[18] investigated the correlation between OCT and VA and found no statistically significant association between VA and the total volume of subretinal fluid or pigment epithelial detachment. Another quantitative subanalysis suggested that increased total volume of the ONL was associated with decreased visual acuity in neovascular AMD.[11] In another trial, decrease in subretinal fluid volume and improvement in BCVA were strongly correlated, but no correlation was found between decreases in retinal and pigment epithelium detachment volumes and improvement in BCVA after three monthly ranibizumab injections.[19] Parravano et al.[20] concluded that intravitreal injections of 0.5 mg ranibizumab were associated with progressive improvement of retinal sensitivity until 24 months, although BCVA values stabilized after 6 months, which suggested that microperimetry may give additional information about macular function that is missed by central VA testing alone.

However, a study found that, in healthy volunteers, the superior retinal sector showed a significantly lower mean sensitivity than did the lower sector because of problems with the illumination of the liquid crystal display monitor inside the MP-1 that might have influenced the results.[8] Our detailed evaluation of the RPE, the IS/OS, and the ELM (Fig. 5) confirmed the results of several studies that reported that both the integrity of the photoreceptor layer[9,10,21,22] and the ELM[23] had a significant correlation with visual function. There are several postulations that refer to a relationship between foveal photoreceptor integrity and preservation of visual function.[22,24] Other SD-OCT parameters, such as mean retinal thickness and central retinal thickness, did not correlate significantly with VA.[21] Considering this information, studies are necessary to determine whether any treatment modality is accompanied by a significant change in retinal function following resolution of fluid, flattening of the PED, and decreasing the NVC, with reintegration of the photoreceptors. We believe treatment indications should be guided more by qualitative morphology and less by quantitative morphology. Optimal treatment success should be evaluated and retreatment decisions should be modified on the basis of morphology and function. Consequently, appropriate methods to identify photoreceptor functional and morphological damage, such as raster scanning SD-OCT with integrated microperimetry, will be of fundamental importance in determining the best treatments.

Acknowledgments

The authors thank Lee M. Jampol for reviewing the manuscript.

References

1. Brown DM, Kaiser PK, Michels M, et al. Ranibizumab versus verteporfin for neovascular age-related macular degeneration. *N Engl J Med*. 2006;355:1432–1444.
2. Rosenfeld PJ, Brown DM, Heier JS, et al. Ranibizumab for neovascular age-related macular degeneration. *N Engl J Med*. 2006;355:1419–1431.
3. Grossniklaus HE, Gass JD. Clinicopathologic correlations of surgically excised type 1 and type 2 submacular choroidal neovascular membranes. *Am J Ophthalmol*. 1998;126:59–69.
4. Freund KB, Zweifel SA, Engelbert M. Do we need a new classification for choroidal neovascularization in age-related macular degeneration? *Retina*. 2010;30:1333–1349.
5. Sayanagi K Sharma S, Yamamoto T, et al. Comparision of spectral-domain versus time-domain optical coherence tomography in management of age-related macular degeneration with ranibizumab. *Ophthalmology*. 2009;116:947–955.
6. Schmidt-Erfurth U, Richard G, Augustin A, et al. Guidance for the treatment of neovascular age-related macular degeneration. *Acta Ophthalmol Scand*. 2007;85:486–494.
7. Springer C, Völcker HE, Rohrschneider K. Statische Fundusperimetrie bei Probanden Microperimeter 1 versus SLO. *Opthalmologe*. 2006;103:214–220.
8. Midena E, Vujosevic S, Cavarzeran F, et al. Normal values for fundus perimetry with the microperimeter MP1. *Ophthalmology*. 2010;117:1571–1576.
9. Charbel Issa P, Troeger E, Finger R, et al. Structure-function correlation of the human central retina. *PloS ONE*. 2010;22: e12864.
10. Landa G, Su E, Garcia P, et al. Inner segment-outer segment junctional layer integrity and corresponding retinal sensitivity in dry and wet forms of age-related macular degeneration. *Retina*. 2011;31:364–370.
11. Kashani AH, Keane PA, Dustin L, et al. Quantitative subanalysis of cystoid spaces and outer nuclear layer using optical coherence tomography in age-related macular degeneration. *Invest Ophthalmol Vis Sci*. 2009;50:3366–3373.

12. Browning DJ, Glassman AR, Aiello LP, et al. Relationship between optical coherence tomography-measured central retinal thickness and visual acuity in diabetic macular edema. *Opthalmology*. 2007;114:525–536.
13. Lalwani GA, Rosenfeld PJ, Fung AE, et al. A variable-dosing regimen with intravitreal ranibizumab for neovascular age-related macular degeneration: year 2 of the PrONTO Study. *Am J Ophthalmol*. 2009;148:43–58.e41.
14. Nilsson UL, Frennesson C, Nilsson SE. Patients with AMD and a large absolute central scotoma can be trained successfully to use eccentric viewing, as demonstrated in a scanning laser ophthalmoscope. *Vision Res*. 2003;43:1777–1787.
15. Calabrese A, Bernard JB, Hoffart L, et al. Wet versus dry age-related macular degeneration in patients with central field loss: different effects on maximum reading speed. *Invest Ophthalmol Vis Sci*. 2011;52:2417–2424.
16. Moutray T, Alarbi M, Mahon G, et al. Relationships between clinical measures of visual function, fluorescein angiographic and optical coherence tomography features in patients with subfoveal choroidal neovascularization. *Br J Ophthalmol*. 2008;92:361–364.
17. Deak G, Bolz M, Ritter M, et al. A systematic correlation of morphology and functional alterations in diabetic macular edema. *Invest Ophthalmol Vis Sci*. 2010;9:50–64.
18. Keane PA, Liakopoulos S, Chang KT, et al. Relationship between optical coherence tomography retinal parameters and visual acuity in neovascular age-related macular degeneration. *Ophthalmology*. 2008;115:2206–2214.
19. Ahlers C, Golbaz I, Stock G, et al. Time course of morphologic effects on different retinal compartments after ranibizumab therapy in age-related macular degeneration. *Ophthalmology*. 2008;115:39–46.
20. Parravano M, Oddone F, Tedeschi M, et al. Retinal functional changes measured by microperimetry in neovascular age-related macular degeneration treated with ranibizumab: 24-months results. *Retina*. 2010;30:1017–1024.
21. Kiss CG, Geitzenauer W, Simader C, et al. Evaluation of ranibizumab-induced changes in high-resolution optical coherence tomographic retinal morphology and their impact on visual function. *Invest Ophthalmol Vis Sci*. 2009;50:2376–2383.
22. Hayashi H, Yamashiro K, Tsujikawa A, et al. Association between foveal photoreceptor integrity and visual outcome in neovascular age-related macular degeneration. *Am J Ophthalmol*. 2009;148:83–89.
23. Oishi A, Hata M, Shimozono M, et al. The significance of external limiting membrane status for visual acuity in age-related macular degeneration. *Am J Ophthalmol*. 2010;150:27–32.
24. Srauss O. The retinal pigment epithelium in visual function. *Physiol Rev*. 2005;85:845–881.